

# Uncertainties on radiation source terms of MINERVA (MYRRHA Phase 1) beam dump

Alexey Stankovskiy<sup>1,\*</sup>, Dario Bisogni<sup>1</sup>, Yurdunaz Çelik<sup>1</sup>, Luca Fiorito<sup>1</sup>, and Gert Van den Eynde<sup>1</sup>

<sup>1</sup>SCK CEN, Boeretang 200, B-2400 Mol, Belgium

**Abstract.** In the framework of Phase I of the MYRRHA project implementation, the superconducting linear accelerator with proton beam parameters 100 MeV, 4 mA is going to be built. To stop the beam, a beam dump based on Al-6061 alloy is designed. The evaluation of radiological impact of an accidental radioactivity release requires the reliable estimates of primary radiation source terms with associated uncertainties. The article addresses the propagation of nuclear data uncertainties through beam dump activation calculations. The Total Monte Carlo approach was used to generate large number of random excitation functions for residual products of proton interactions with materials of Al-6061 alloy. The residual products do not impose any feedback on proton and neutron spectra in the beam dump, moreover the calculation of the production rates is sufficient to obtain uncertainties on final activities. This significantly accelerates the uncertainty quantification allowing to study the convergence of mean and higher moments (variance, variance of variance) for individual nuclides.

## 1 Introduction

The Multi-purpose hYbrid Research Reactor for High-tech Applications, MYRRHA, is being designed at SCK CEN since 1998 [1]. A detailed implementation strategy features a phased approach in order to reduce the technical risk, to spread the investment cost and to allow a first R&D facility available by 2026. As detailed in [2], in this new approach the MYRRHA facility will start with the 100 MeV accelerator (phase 1) and will be followed by the 100-600 MeV accelerator section (phase 2) and by the reactor (phase 3). At the level of the proton accelerator the first phase consists of building and operating the linac limited to 100 MeV final beam energy. It is well known that beam reliability is the main challenge of the ADS driver. In MYRRHA's case this challenge is expressed as a beam-MTBF (Mean Time Between Failures) of 250 hours. Hence, the principle aim of phase 1 is to experimentally investigate the feasibility and efficiency of the reliability and fault tolerance schemes that are envisaged for the 600 MeV linac. Also in phase 1 it is foreseen to transport a  $\sim 10\%$  fraction of the 100 MeV beam to a target station for innovative medical radioisotopes production by an Isotope Separation On-Line (ISOL) technique. MINERVA (MYRRHA Isotopes Production coupling the linEar acceleRator to the Versatile proton target fAcility) is the name of the project that combines the phase 1 100 MeV linac, the ISOL target station, the target station for fusion materials research and all the associated services and buildings. Among many parameters, design optimization for MINERVA depends on the accuracy of radiological assessment of the unmitigated accidental release. The Best Estimate Plus Uncertainty analysis (BEPU) option

[3] is recommended by IAEA to assess the consequences of postulated initiating events (PIEs). At the design stage of MINERVA, it is possible to propagate only basic design uncertainties to the quantities of interest which are in this case primary radiation source terms. In view of absence of information on uncertainties in material compositions, geometrical dimensions, beam performance, etc., the only type of uncertainty that can be propagated to primary radiation source terms is nuclear data uncertainty, i.e. uncertainty associated to the residual nuclei production cross sections describing interactions of primary protons and secondary particles (mostly neutrons) with matter. The article addresses the uncertainty quantification for the beam dump designed to absorb full-intensity 4 mA beam of 100 MeV protons.

## 2 Residual production cross sections

To fully stop the 4-mA beam of 100 MeV protons, a solid beam dump is going to be installed at the end of the beam line. The schematic view of the beam dump is shown in Figure 1. The core of the beam dump is composed of a set of disks attached together to form a conical structure to spread the heat load from the proton beam uniformly in the depth. The disks are made of Al-6061 alloy which is composed predominantly by Al (97.2 wt.% on average), as well as Mg, Si, Ti, Cr, Mn, Fe, Cu, Zn with weight fractions ranging from 0.1 to 0.6%. These elements therefore cannot be treated as impurities and one may expect significant contribution of their radioactive products from proton- and neutron-induced interactions into the total primary source term (i.e activity). In the Table 1 the dominant contributors into the effective inhalation dose to a critical individual at critical point are listed. In the right-hand

\*e-mail: alexey.stankovskiy@sckcen.be

**Table 1.** Main contributors into the inhalation dose from unmitigated release for 1 year old individual at a distance of 550 meters [4]

Nuclide	Dose, mSv	main production channel
$^{22}\text{Na}$	10.3	$^{27}\text{Al}(p,x)$
$^{24}\text{Na}$	2.55	$^{27}\text{Al}(p,x)$
$^{54}\text{Mn}$	0.22	$^{56}\text{Fe}(p,x)$
$^{56}\text{Co}$	0.20	$^{56}\text{Fe}(p,x)$
$^{18}\text{F}$	0.17	$^{27}\text{Al}(p,x)$
$^{48}\text{V}$	0.15	$^{52}\text{Cr}(p,x)$
$^{65}\text{Zn}$	0.11	$^{66}\text{Zn}(p,x)$
$^{55}\text{Fe}$	0.10	$^{56}\text{Fe}(p,x)$
$^{46}\text{Sc}$	0.10	$^{48}\text{Ti}(p,x)$
$^{52}\text{Mn}$	0.08	$^{56}\text{Fe}(p,x)$
$^{27}\text{Mg}$	0.07	$^{27}\text{Al}(n,x)$
$^{58}\text{Co}$	0.06	$^{63}\text{Cu}(p,x)$
$^{60}\text{Co}$	0.04	$^{63}\text{Cu}(p,x)$
$^{57}\text{Co}$	0.02	$^{63}\text{Cu}(p,x)$
$^7\text{Be}$	0.02	$^{27}\text{Al}(p,x)$

column, the principal nuclear reaction producing given nuclide in the beam dump material continuously during irradiation is specified.

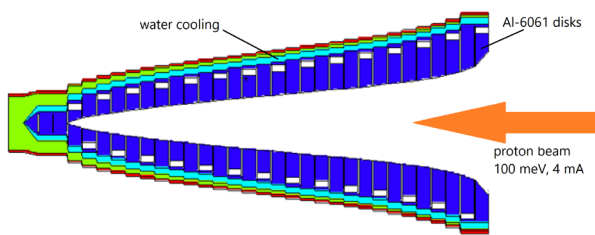


**Figure 1.** Schematic view of the MINERVA beam dump

The majority of nuclides is produced from proton-induced interactions. However,  $^{27}\text{Mg}$  for example is produced by neutrons. Some lower contributors, which are not listed in the table but have nevertheless a non-negligible activity, such as  $^{64}\text{Cu}$  and  $^{24m}\text{Na}$ , are also produced mainly by neutron reactions.

To propagate nuclear data uncertainty it was decided to use the Total Monte Carlo (TMC) method [5], which relies on the TALYS nuclear reaction code to produce cross section data. The method consists in sampling the TALYS input parameters from probability distributions constructed from the analysis of experimental data. Each sampled input dataset is used to run TALYS and produce associated perturbed cross sections. All the process is fully automated in the T6 software [5], the latest version of which has been used for this study. The core of the T6 suite is the TALYS nuclear reaction code, which is coupled to other utilities that perform the analysis of experimental data, random sampling, formatting in ENDF-6 format, etc. From the huge amount of data printed out after T6 runs, only randomly sampled excitation functions (or energy-dependent residual production cross sections) are actually needed to propagate the uncertainties for the ra-

diation source terms. To cover all the major contributors to the dose listed in Table 1, 500 randomly sampled files containing information on all energy-dependent residual production cross sections have been created for each of the following nuclides:  $^{27}\text{Al}$ ,  $^{48}\text{Ti}$ ,  $^{52}\text{Cr}$ ,  $^{56}\text{Fe}$ ,  $^{63}\text{Cu}$ , and  $^{66}\text{Zn}$ , both for proton- and neutron-induced interactions. The excitation functions for two major dose contributors,  $^{22}\text{Na}$  and  $^{24}\text{Na}$ , are plotted in Figure 2 against experimental data.

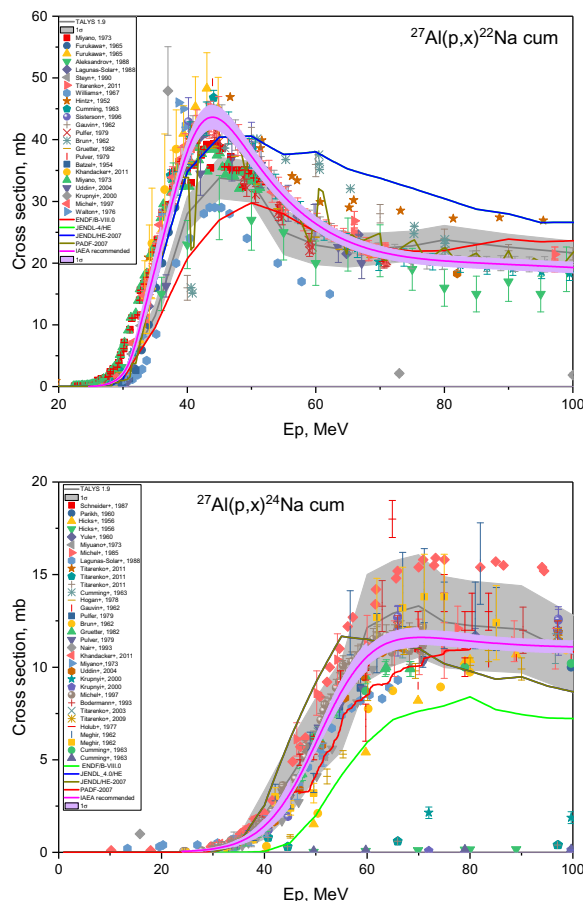


**Figure 2.** Excitation functions  $^{27}\text{Al}(p,x)^{22}\text{Na}$  and  $^{27}\text{Al}(p,x)^{24}\text{Na}$ . Experimental data are taken from EXFOR database [6]

Shown in gray are the results of T6 calculations (central values over 500 samples and one standard deviation uncertainty band). In addition, the data represented by magenta curve along with its  $1\sigma$  uncertainty is taken from the IAEA collection of reference proton-induced reactions [7]. However, this IAEA recommended values (uncertainty bands) do not cover the experimental data, even if one extends them to  $2\sigma$  or even  $3\sigma$ , while the T6 calculated uncertainties, being extended to 95% or 99% confidence intervals, cover all the experimental data with their associated experimental errors. To obtain conservative estimates of the  $^{22}\text{Na}$  and  $^{24}\text{Na}$  activities and associated uncertainties, the T6 generated excitation functions were used, despite of the availability of IAEA reference cross sections.

Although TALYS is considered nowadays as the most powerful nuclear reaction code, it has deficiencies in treating some reaction channels. For instance, it cannot adequately reproduce emission of light nuclei such as  ${}^7\text{Be}$ , which is listed in Table 1 among the major contributors into the dose. Preequilibrium and statistical models of TALYS consider  ${}^7\text{Be}$  as a residual nucleus in the output channel of the reaction. However,  ${}^7\text{Be}$  can be also formed as pickup of  ${}^3\text{He}$  and  ${}^4\text{He}$ , emitted from excited compound nucleus, but not yet left the nucleus. To model that, coalescence pick-up models are used in dedicated codes such as ALICE/ASH [8]. Therefore, the  ${}^7\text{Be}$  production cross section from  ${}^{27}\text{Al}$  has been taken from the KIT report [9] together with its  $1\sigma$  uncertainty band. In this report, the  ${}^7\text{Be}$  production cross sections were obtained using modified ALICE/ASH code for all stable nuclei from Carbon to Bismuth. The data in [9] are provided with associated standard deviations, therefore, for this particular reaction, the separate sampling was performed using the diagonal elements of covariance matrix. The plot of the  ${}^{27}\text{Al}(p,x){}^7\text{Be}$  excitation function is shown in Figure 3.

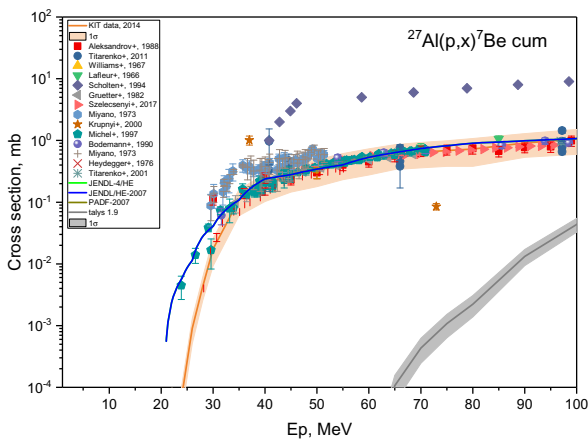


**Figure 3.** Excitation function  ${}^{27}\text{Al}(p,x){}^7\text{Be}$

As it is seen, the T6-based excitation function has much lower values than all the experimental data. The reason behind this is that this cross section is the sum of partial reaction cross sections  ${}^7\text{Be}+n+5\alpha$ ,  ${}^7\text{Be}+d+t+4\alpha$ , and  ${}^7\text{Be}+2t+{}^3\text{He}+3\alpha$ , with the minimum threshold among them being 47 MeV for the  ${}^7\text{Be}+n+5\alpha$  reaction. These reactions are much less likely to occur than the pickup of  ${}^3\text{He}$  by  ${}^4\text{He}$  which energetically opens at 20 MeV. The KIT data [9] are definitely more reliable for this particular reaction.

### 3 Uncertainties on radiation source terms

The randomly sampled excitation functions from proton- and neutron-induced interactions generated for the nuclides listed in Section 2 were written into ALEPH2 format [10] and plugged into ALEPH2 depletion calculation. The proton- and neutron-induced spectra obtained during reference activation calculation for the beam dump core

were used. Obviously, in contrast to fission products in the reactor fuel, there is no feedback of activation products on the proton and neutron spectra and therefore the TMC method which may face difficulties regarding computational time and memory consumption in case of reactor simulations, perfectly suits to propagate uncertainties in the case of accelerator radiation source terms. Moreover, a very accurate convergence of the mean and variance may be achieved by running a high number of samples. In this task, from the analysis of the available hardware resources and time, it was decided to obtain the uncertainties from the statistical analysis of 500 independent runs of ALEPH2 code.

It must be also noted that the ALEPH2 runs were limited to the calculations of reaction rates only. It was not necessary to perform full depletion calculation for the whole irradiation and decay history. ALEPH2, as any other depletion code, is solving the system of ordinary differential equations for nuclide concentrations  $N$

$$\begin{aligned} \frac{d\vec{N}(t)}{dt} &= \hat{A}\vec{N}(t) \\ \vec{N}(t = t_0) &= \vec{N}_0 \end{aligned} \quad (1)$$

with the coefficients of matrix  $\hat{A}$

$$a_i = \sum_m \langle \sigma_i^m \rangle \langle \varphi^m \rangle + \lambda_i \quad (2)$$

(diagonal elements defining removal of nuclide  $i$ ) and

$$a_{ji} = \sum_m \langle \sigma_{ji}^m \rangle \langle \varphi^m \rangle + \lambda_{ji} \quad (3)$$

(off-diagonal elements defining production of nuclide  $i$  from nuclides  $j$ ).

Here index  $m$  runs from 1=proton to 2=neutron;  $\langle \sigma_{ji}^m \rangle$  is the spectrum-averaged cross section of the process (removal in case of sole index  $i$  or production from nuclide  $j$ ),  $\langle \varphi^m \rangle$  is the particle flux, and  $\lambda$  is the decay constant.

If at the first approximation to neglect the production of nuclide  $i$  from all but parent nuclide  $j$ , one may reduce the system to a single equation

$$\frac{dN_i}{dT} = I \cdot Y_i - \lambda_i N_i \quad (4)$$

Here  $I$  is the proton beam current and  $Y_i = \sum_j Y_{ji}$  is the nuclide yield from parent nuclide per one incident proton. The term  $I \cdot Y_i$  can always be obtained from reaction rates as

$$I \cdot Y_i = \sum_j N_j \cdot \sum_m \langle \sigma_{ji}^m \rangle \langle \varphi^m \rangle \quad (5)$$

The solution of above differential equation directly in terms of activities  $A_i$  is

$$A_i = \lambda_i N_i(t) = I \cdot Y_i \cdot (1 - e^{-\lambda_i t}) \cdot e^{-\lambda_i t} \quad (6)$$

Therefore, assuming that the uncertainties on decay constants are low compared to the cross section uncertainties,

**Table 2.** Uncertainties on the activities of main contributors into the inhalation dose

Nuclide	Relative uncertainty $1\sigma$ (%)
$^{22}\text{Na}$	10.9
$^{24}\text{Na}$	14.0
$^{54}\text{Mn}$	18.3
$^{56}\text{Co}$	11.9
$^{18}\text{F}$	16.8
$^{48}\text{V}$	8.0
$^{65}\text{Zn}$	8.2
$^{55}\text{Fe}$	9.0
$^{46}\text{Sc}$	14.8
$^{52}\text{Mn}$	9.3
$^{27}\text{Mg}$	13.3
$^{58}\text{Co}$	20.3
$^{60}\text{Co}$	29.5
$^{57}\text{Co}$	13.3
$^7\text{Be}$	17.8

the perturbation of the final activity will be directly proportional to the perturbation of the product yield

$$\delta A_i = \delta(I \cdot Y_i \cdot (1 - e^{-\lambda_i t}) \cdot e^{-\lambda_i t}) \sim \delta Y_i \quad (7)$$

In other words, the uncertainties on the final activities are determined by the uncertainties on the reaction rates. Therefore it is sufficient to sum up the uncertainties on proton- and neutron-induced reaction rates at the beginning of irradiation to get the final uncertainty on actinide activity.

The resulting uncertainties for the major contributors to the dose are listed in Table 2.

The plots on Figure 4 demonstrate how the uncertainties are converging with the number of TMC samples. It is interesting to observe that  $^{60}\text{Co}$  with its highest uncertainty among major contributors to the dose listed in Table 2 also converges rather poorly, compared to other nuclides. Nevertheless, the 500 samples must be deemed satisfactory for the purpose of present study.

## 4 Conclusions

The uncertainties for the nuclide activities produced in the Al-6061 beam dump core due to nuclear data uncertainties have been assessed using Total Monte Carlo method propagating randomized nuclide production cross section data through activation calculations with subsequent statistical analysis of the results. The uncertainties on the most important nuclide activities are in the range 8-30 %. To get reliable uncertainty estimates, one need to run at least several hundreds of randomly sampled files with excitation functions leading to the production of nuclides of interest.

## References

[1] H. Ait Abderrahim et al., Nuclear Physics News **20**, No. 1, p. 24-28 (2010)

[2] D. De Bruyn et al., Proc. 2018 International Congress on Advances in Nuclear Power Plants (ICAPP'18), Charlotte, North Carolina, USA, pp. 1066-1073 (2018)  
 [3] IAEA *Safety Standards* (SSG-2 IAEA, 2009)  
 [4] Y. Çelik and A. Stankovskiy, SCK CEN/34139446 (2019)  
 [5] A.J. Koning and D. Rochman, Nucl. Data Sheets **113**, p. 2841 (2012)  
 [6] Experimental Nuclear Reaction Data (EXFOR), <https://www-nds.iaea.org/exfor/exfor.htm>  
 [7] A. Hermanne et al., Nucl. Data Sheets **148**, p. 338-382 (2018)  
 [8] C.H.M. Broeders et al., Report FZKA 7183, May 2006, <http://bibliothek.fzk.de/zb/berichte/FZKA7183.pdf>  
 [9] A. Yu. Konobeyev and U. Fischer, KIT Scientific Reports 7684 (2014)  
 [10] A. Stankovskiy and G. Van den Eynde, Sci. Technol. Nucl. Install, p. 545103 (2012)

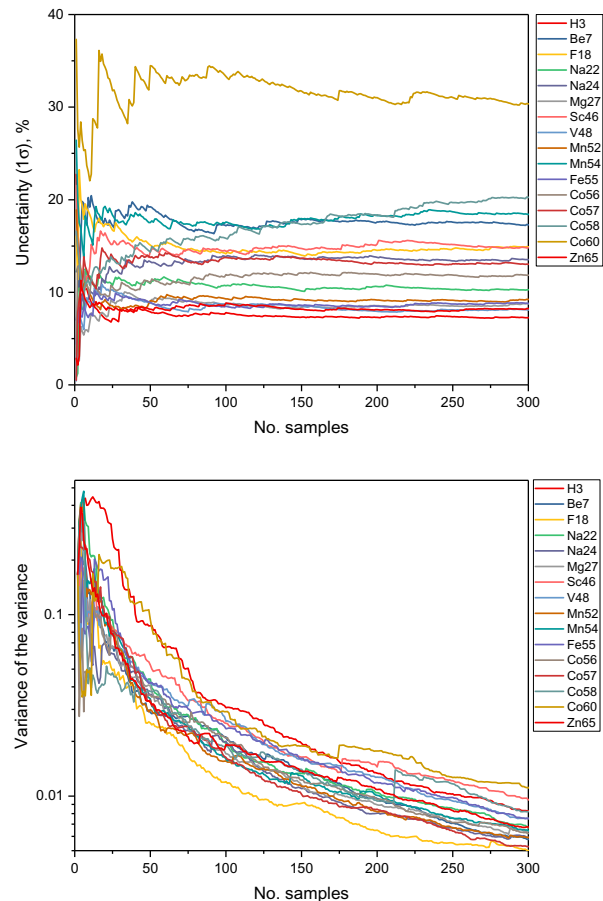


**Figure 4.** Convergence of the variance